

Supporting Information

Effect of steric changes on the isoselectivity of dinuclear indium catalysts for lactide polymerization

Kimberly M. Osten, Dinesh C. Aluthge, Parisa Mehrkhodavandi*

Department of Chemistry, University of British Columbia, 2036 Main Mall, Vancouver, BC V6T 1Z1, Canada.

Table of Contents

A. Characterization of compounds by ¹H NMR spectroscopy	4
Figure S1. ¹ H NMR spectrum (600 MHz, 25 °C, CDCl ₃) of proligand (±)-H(NNO _{SiPh₃}).	4
Figure S2. ¹ H NMR spectrum (600 MHz, 25 °C, CDCl ₃) of proligand (±)-H(NNO _{Ad}).	5
Figure S3. ¹ H NMR spectrum (600 MHz, 25 °C, CDCl ₃) of proligand (±)-H(NNO _{Cm}).	6
Figure S4. ¹ H NMR spectra (600 MHz, 25 °C, CD ₂ Cl ₂) of complexes (a) (±)- 1 and (b) (<i>R,R</i>)- 1	7
Figure S5. ¹ H NMR spectra (600 MHz, 25 °C, CD ₂ Cl ₂) of complexes (a) (±)- 2 and (b) (<i>R,R</i>)- 2	7
Figure S6. ¹ H NMR spectra (600 MHz, 25 °C, CD ₂ Cl ₂) of complexes (a) (±)- 3 and (b) (<i>R,R</i>)- 3	8
Figure S7. ¹ H NMR spectrum (600 MHz, 25 °C, CDCl ₃) of complex (±)- 4	9
Figure S8. ¹ H NMR spectrum (600 MHz, 25 °C, CDCl ₃) of complex (±)- 5	10
Figure S9. ¹ H NMR spectrum (600 MHz, 25 °C, CDCl ₃) of complex (±)- 6	11
B. Characterization of compounds by PGSE NMR spectroscopy.....	12
Figure S10. Plots of ln(I/I ₀) vs. $\gamma^2\delta^2G^2[\Delta-(\delta/3)] \times 10^{10}$ (m ⁻² s) from PGSE NMR experiments (400 MHz, CD ₂ Cl ₂ , 25 °C) for complex (±)- 4 (red), complex (±)- 1 (orange), complex (<i>R,R</i>)- 1 (yellow), complex (±)- 2 (green), proligand (±)-H(NNO _{SiPh₃}) (blue), proligand (±)-H(NNO _{Ad}) (purple) and internal standard tetrakis(trimethylsilyl)silane (TMSS) (black).	12
C. Characterization of compounds in the solid-state.....	14
Table S1. Crystallographic parameters of complexes 1 , 2 , 5 and 6	14
D. Kinetic studies of the polymerization of lactide by catalysts 4-6.....	15
Figure S11. Plots of the ln([LA]) vs. time for the polymerization of <i>rac</i> -, L- and D-LA (0.5 M) by complex (±)- 4 (2.4 mM) monitored to >97% conversion by ¹ H NMR spectroscopy in CDCl ₃ and CD ₂ Cl ₂ with 1,3,5-trimethoxybenzene used as an internal standard (0.03 M).	15
Figure S12. Plots of the ln([LA]) vs. time for the polymerization of <i>rac</i> -, L- and D-LA (0.5 M) by complex (<i>R,R</i>)- 4 (2.4 mM) monitored to >86% conversion by ¹ H NMR spectroscopy in CDCl ₃ and CD ₂ Cl ₂ with 1,3,5-trimethoxybenzene used as an internal standard (0.03 M).	15
Figure S13. Plots of the ln([LA]) vs. time for the polymerization of <i>rac</i> -, L- and D-LA (0.5 M) by complex (±)- 5 (2.4 mM) monitored to >98% conversion by ¹ H NMR spectroscopy in CDCl ₃ with 1,3,5-trimethoxybenzene used as an internal standard (0.03 M).	16
Figure S14. Plots of the ln([LA]) vs. time for the polymerization of <i>rac</i> -, L- and D-LA (0.5 M) by complex (<i>R,R</i>)- 5 (2.4 mM) monitored to >80% conversion by ¹ H NMR spectroscopy in CDCl ₃ with 1,3,5-trimethoxybenzene used as an internal standard (0.03 M).	16
Figure S15. Plots of the ln([LA]) vs. time for the polymerization of <i>rac</i> -, L- and D-LA (0.5 M) by complex (±)- 6 (2.4 mM) monitored to >98% conversion by ¹ H NMR spectroscopy in CDCl ₃ with 1,3,5-trimethoxybenzene used as an internal standard (0.03 M).	17

E. *In situ* ¹H NMR spectroscopy of the polymerization of lactide by catalysts 4-6..... 18

Figure S16. ¹H NMR spectra (400 MHz, CDCl₃, 25 °C) of (a) complex (±)-**1**, (b) complex (±)-**4**, (c) the polymerization of *rac*-LA (0.48 M) by complex (±)-**4** (2.4 mM) in CDCl₃ monitored *in situ* in an NMR tube to 97% conversion with 1,3,5-trimethoxybenzene (TMB) used as an internal standard and (d) the polymerization of *rac*-LA (~0.5 M) by complex (±)-**4** (~2 mM) which was stirred at room temperature in CDCl₃ for 2 hours before being analyzed by NMR spectroscopy (98% conversion). The blue dots denote peaks coincident with (±)-**4**, the red dots denote peaks coincident with (±)-**1** and the green dots denote the indium polymeryl species.....**18**

Figure S17. ¹H NMR spectra (400 MHz, CD₂Cl₂, 25 °C) of (a) complex (±)-**1**, (b) complex (±)-**4** and the polymerization of *rac*-LA (0.48 M) by complex (±)-**4** (2.4 mM) in CD₂Cl₂ monitored *in situ* in an NMR tube with 1,3,5-trimethoxybenzene (TMB) used as an internal standard at 1% (c) and 97% (d) conversion. The blue dots denote peaks coincident with (±)-**4**, the red dots denote peaks coincident with (±)-**1** and the green dots denote the indium polymeryl species.**18**

Figure S18. ¹H NMR spectra (400 MHz, CDCl₃, 25 °C) of (a) complex (±)-**2**, (b) complex (±)-**5** and the polymerization of *rac*-LA (0.48 M) by complex (±)-**5** (2.4 mM) in CDCl₃ monitored *in situ* in an NMR tube with 1,3,5-trimethoxybenzene (TMB) used as an internal standard at 29% (c) and 97% (d) conversion. The blue dots denote peaks coincident with (±)-**5** and the green dots denote the indium polymeryl species.....**19**

Figure S19. ¹H NMR spectra (400 MHz, CDCl₃, 25 °C) of (a) complex (±)-**3**, (b) complex (±)-**6** and the polymerization of *rac*-LA (0.48 M) by complex (±)-**6** (2.4 mM) in CDCl₃ monitored *in situ* in an NMR tube with 1,3,5-trimethoxybenzene (TMB) used as an internal standard at 29% (c) and 97% (d) conversion. The blue dots denote peaks coincident with (±)-**6** and the green dots denote the indium polymeryl species.....**19**

Figure S20. ¹H NMR spectra (400 MHz, CDCl₃, 25 °C) of (a) complex (±)-(NNO_{*t*Bu})InCl₂, (b) complex (±)-[(NNO_{*t*Bu})InCl]₂(μ-Cl)(μ-OEt) and the polymerization of *rac*-LA (0.48 M) by complex (±)-[(NNO_{*t*Bu})InCl]₂(μ-Cl)(μ-OEt) (2.4 mM) in CDCl₃ monitored *in situ* in an NMR tube with 1,3,5-trimethoxybenzene (TMB) used as an internal standard at 29% (c) and 97% (d) conversion. The blue dots denote peaks coincident with (±)-[(NNO_{*t*Bu})InCl]₂(μ-Cl)(μ-OEt) and the green dots denote the indium polymeryl species.**20**

F. Fully-labelled ORTEP diagrams of solid state structures of complexes 1, 2, 5, and 6.. 20

G. References..... 22

A. Characterization of compounds by ^1H NMR spectroscopy

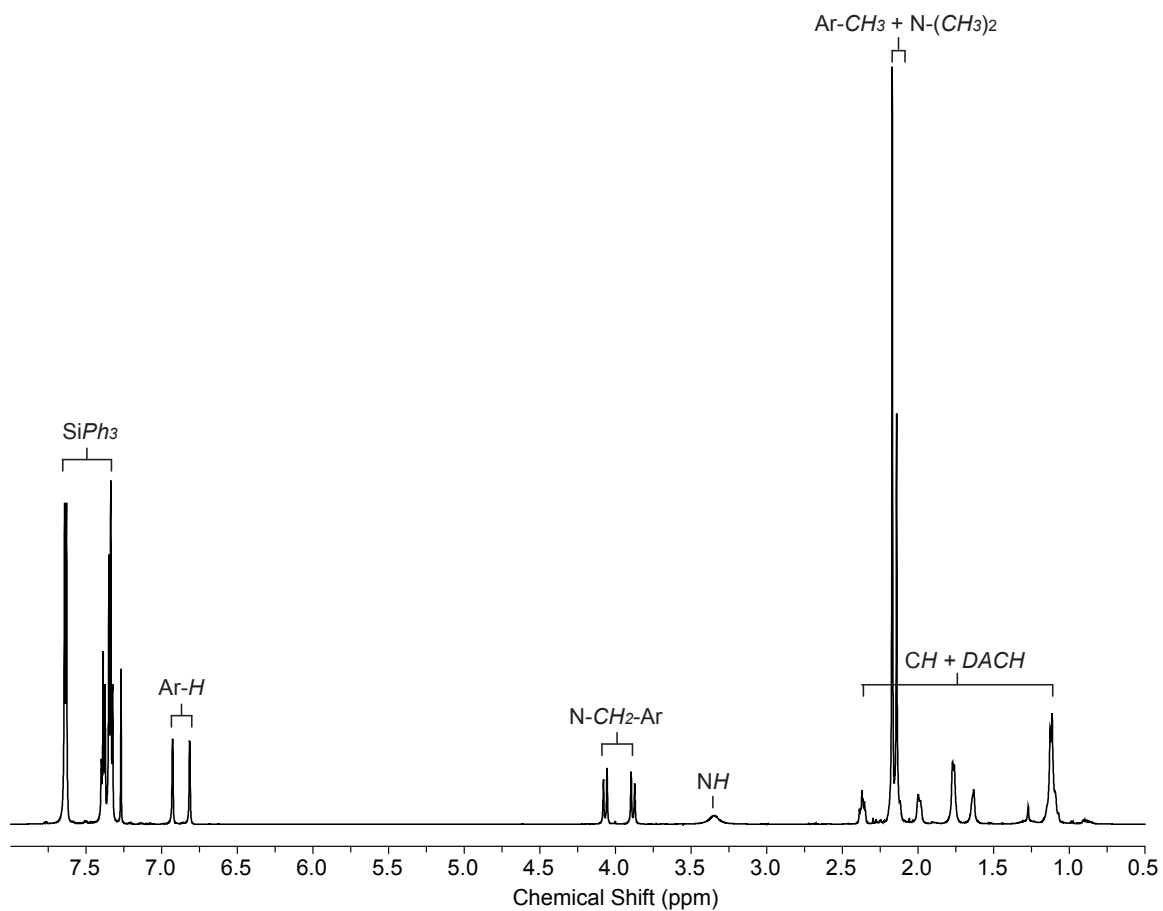


Figure S1. ^1H NMR spectrum (600 MHz, 25 °C, CDCl_3) of proligand $(\pm)\text{-H(NNO}_{\text{SiPh}_3})$.

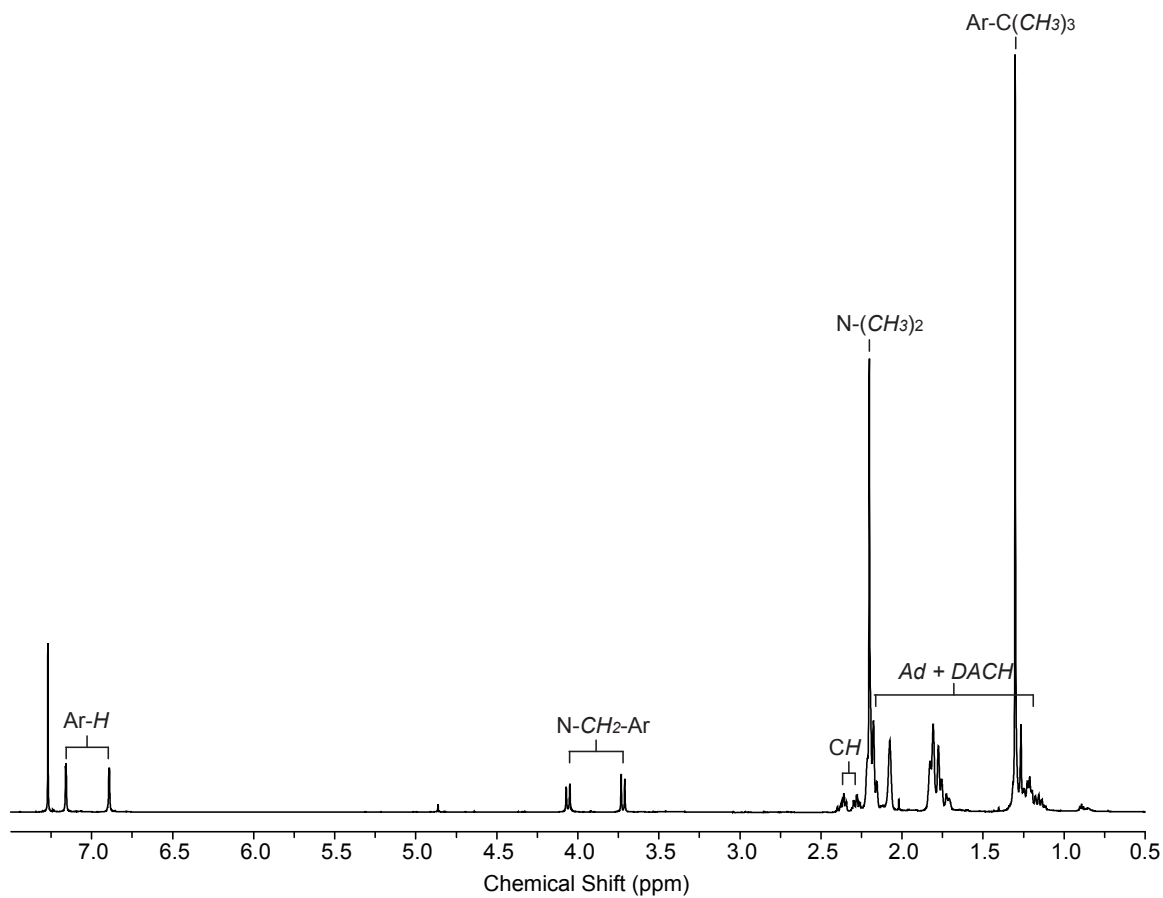


Figure S2. ^1H NMR spectrum (600 MHz, 25 °C, CDCl_3) of proligand $(\pm)\text{-H(NNO}_{\text{Ad}})$.

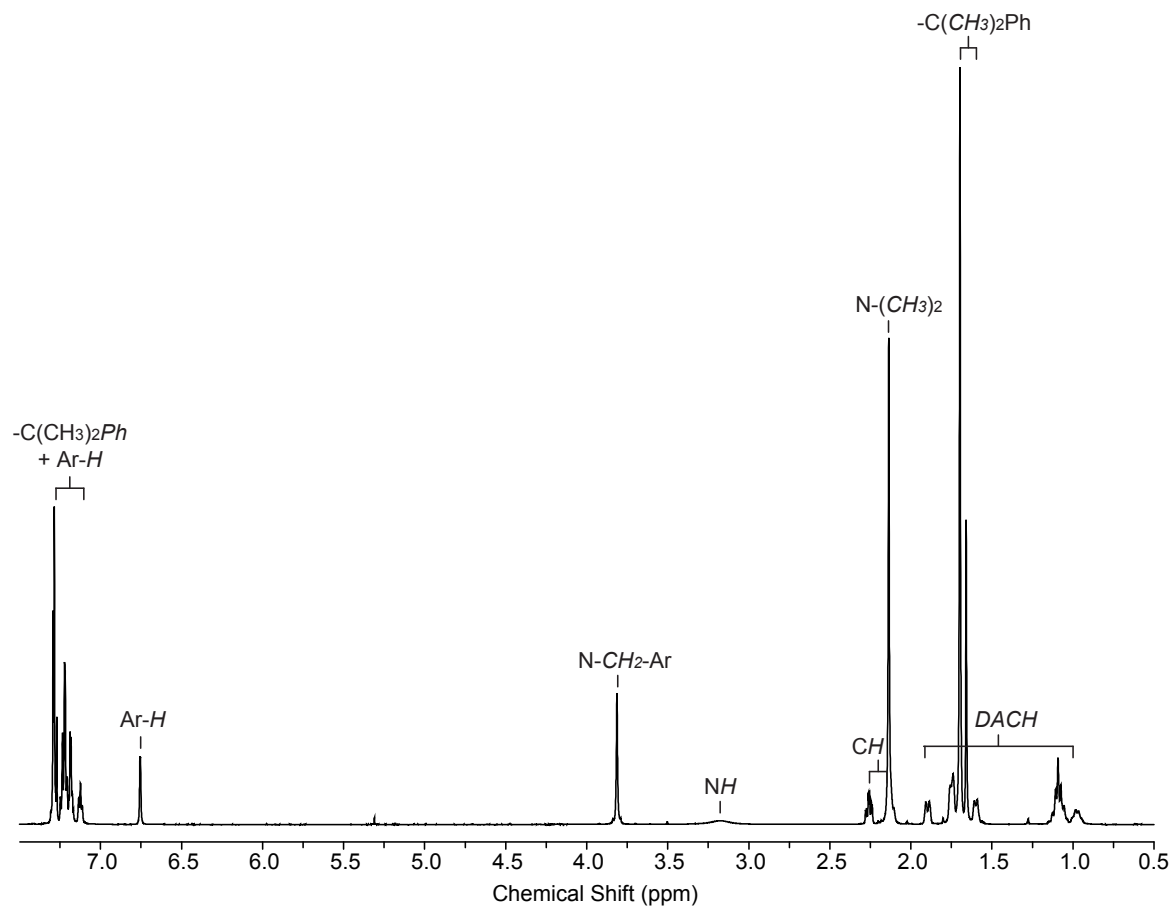


Figure S3. ^1H NMR spectrum (600 MHz, 25 °C, CDCl_3) of proligand $(\pm)\text{-H(NNO}_{\text{cm}})$.

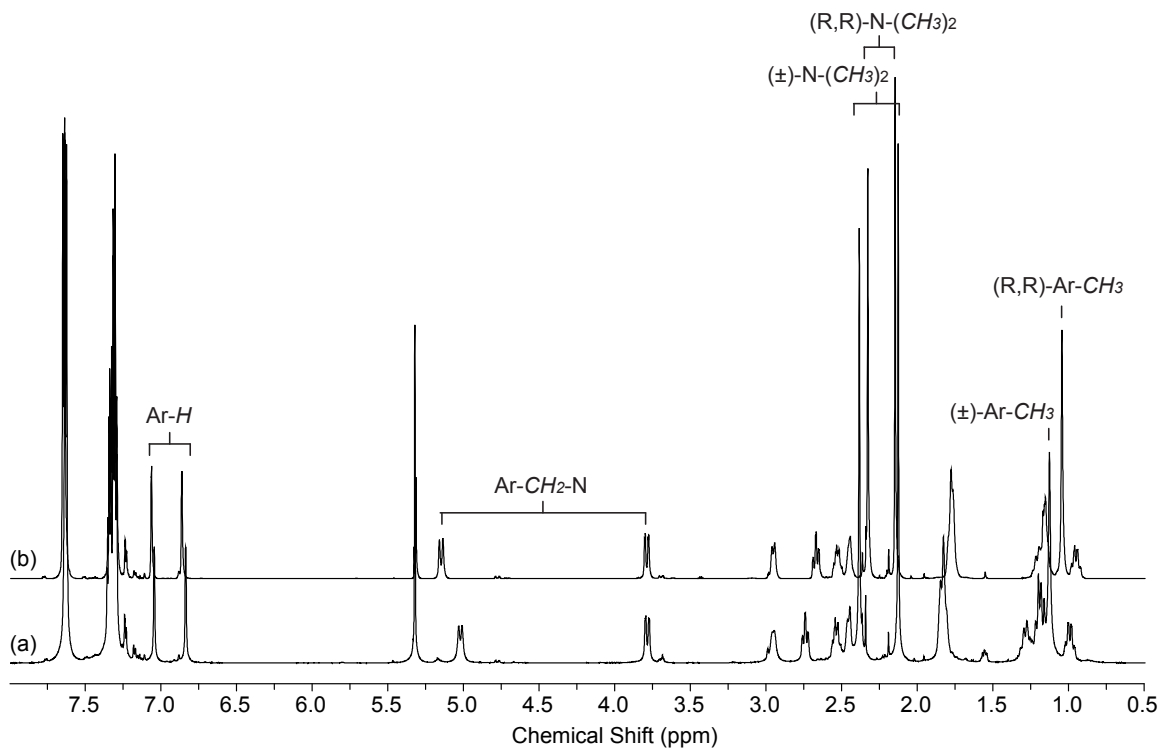


Figure S4. ^1H NMR spectra (600 MHz, 25 °C, CD_2Cl_2) of complexes (a) (\pm) -**1** and (b) (R,R) -**1**.

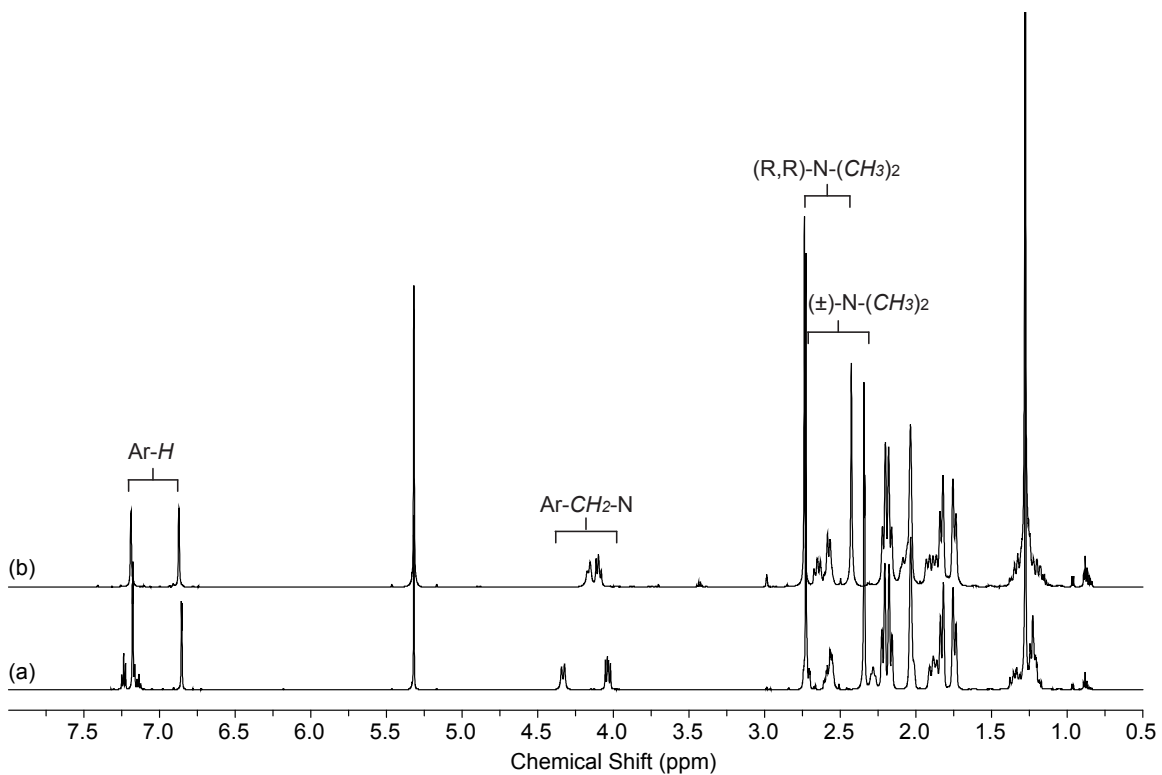


Figure S5. ^1H NMR spectra (600 MHz, 25 °C, CD_2Cl_2) of complexes (a) (\pm) -**2** and (b) (R,R) -**2**.

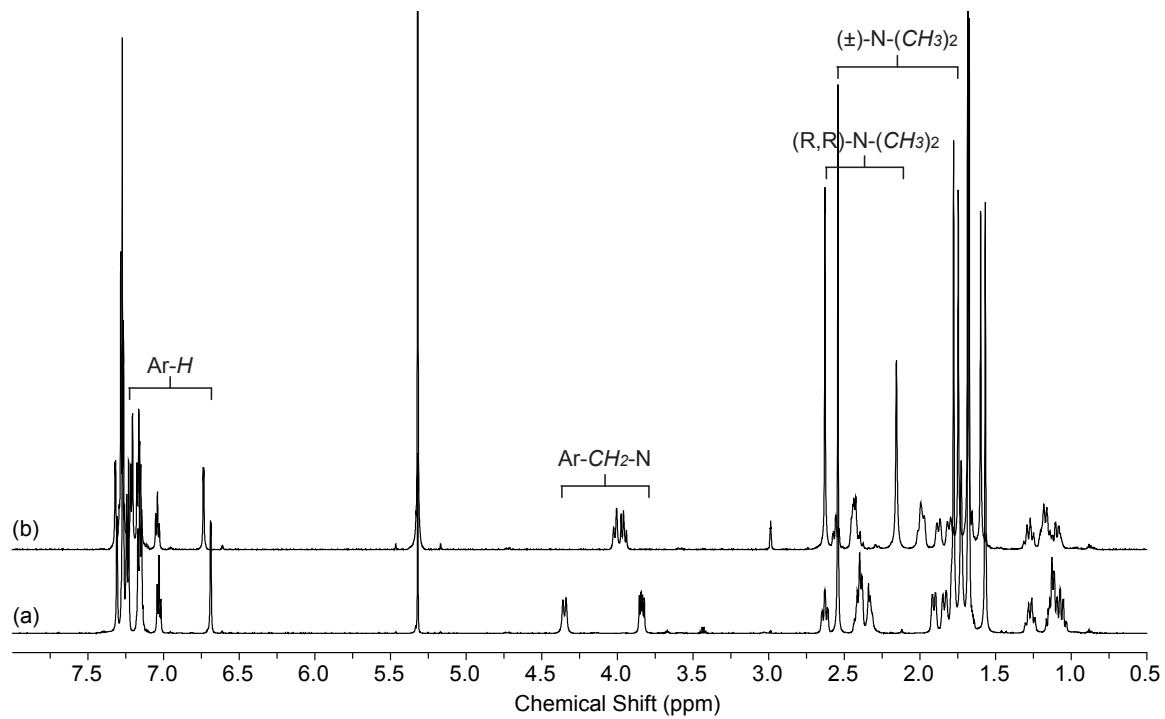


Figure S6. ¹H NMR spectra (600 MHz, 25 °C, CD₂Cl₂) of complexes (a) (±)-**3** and (b) (R,R)-**3**.

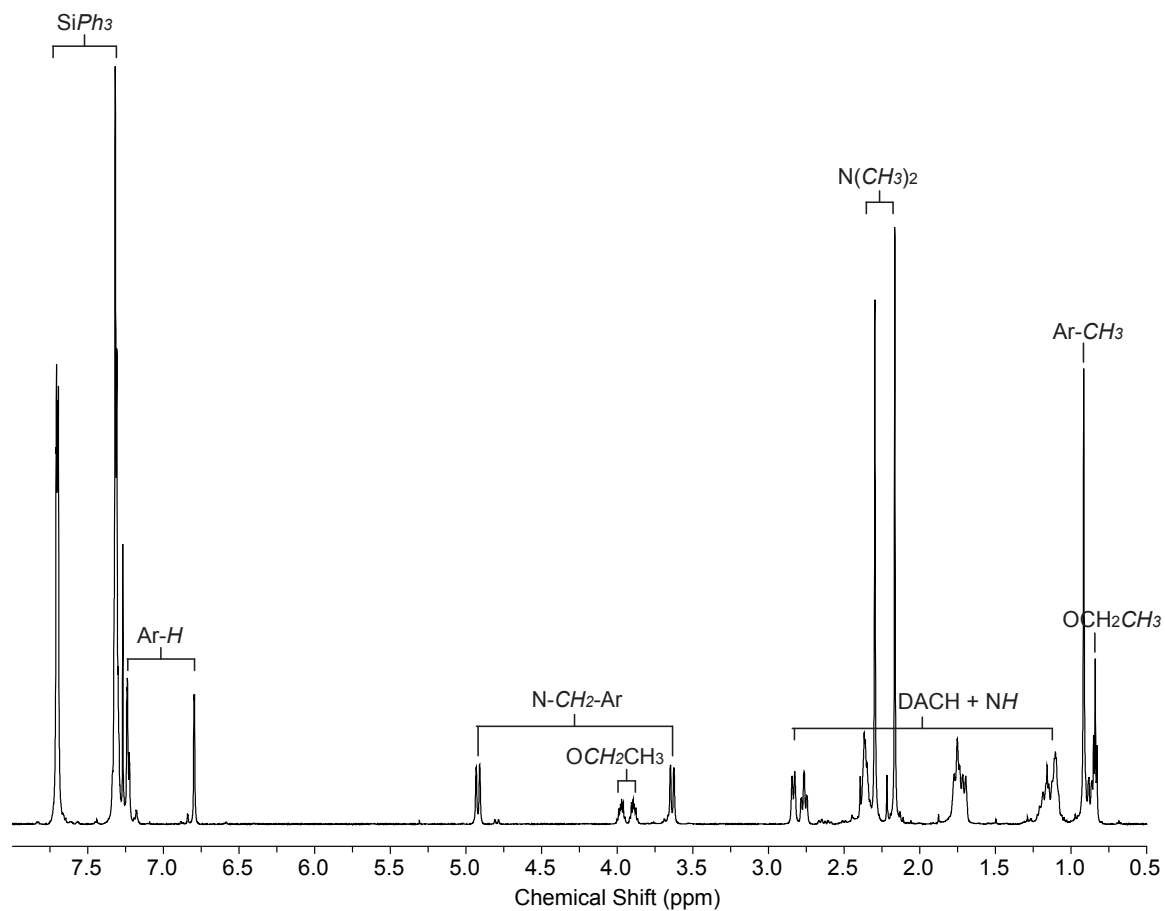


Figure S7. ^1H NMR spectrum (600 MHz, 25 °C, CDCl_3) of complex (\pm)-4.

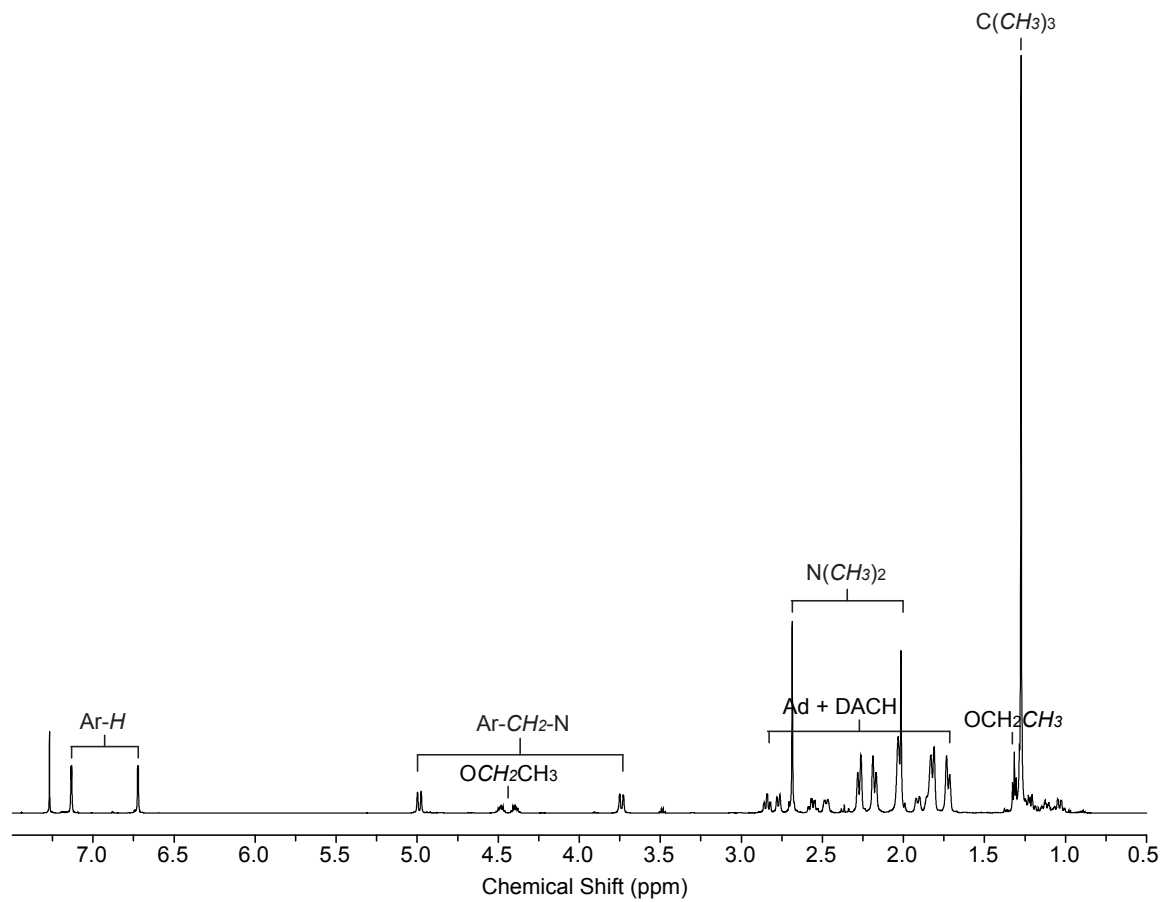


Figure S8. ^1H NMR spectrum (600 MHz, 25 °C, CDCl_3) of complex (\pm) -5.

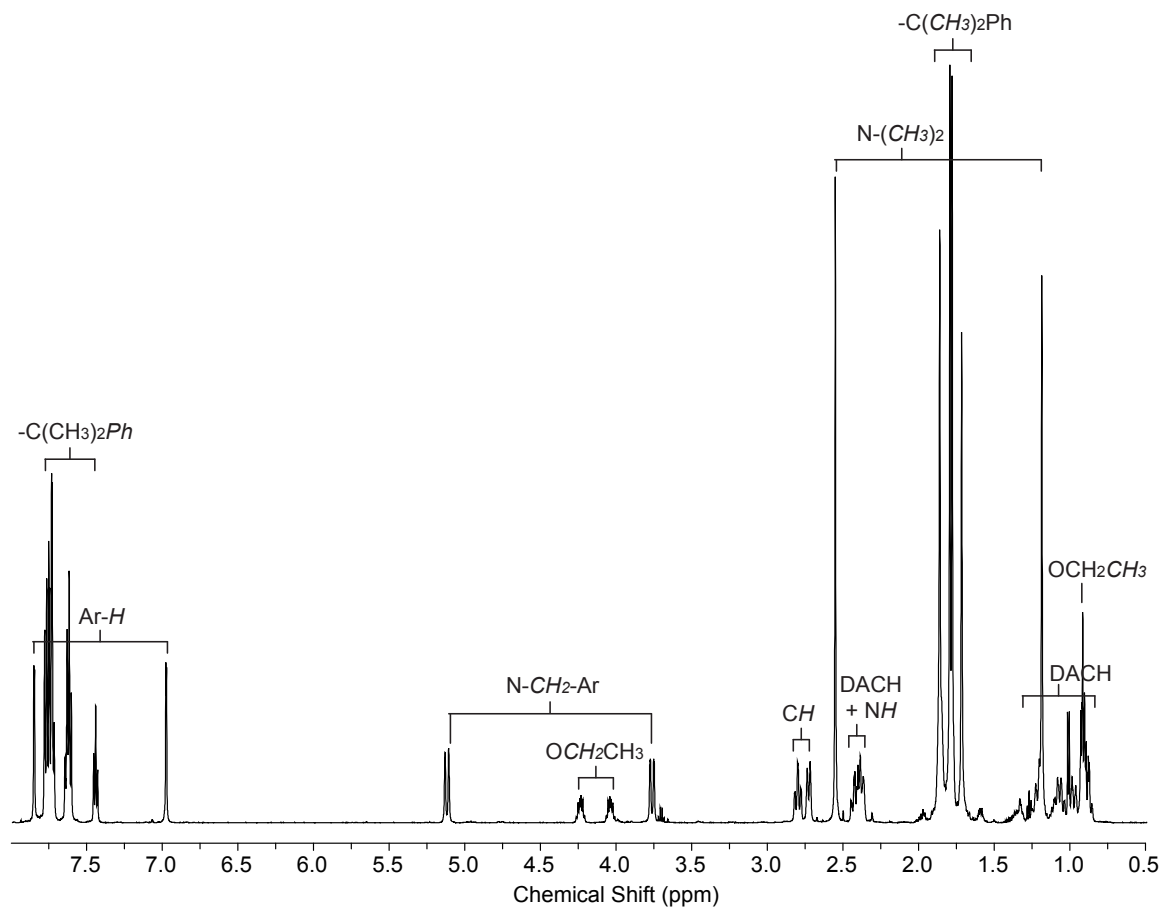


Figure S9. ^1H NMR spectrum (600 MHz, 25 °C, CDCl_3) of complex (\pm)-6.

B. Characterization of compounds by PGSE NMR spectroscopy

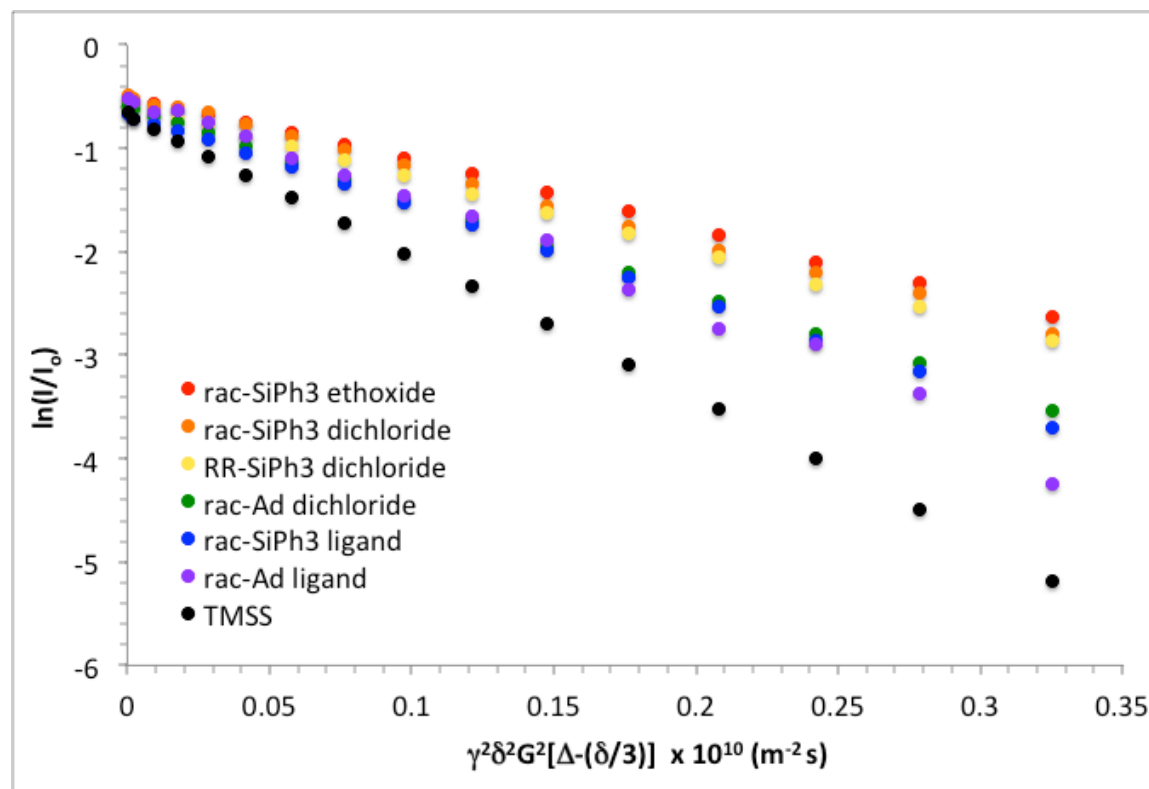


Figure S10. Plots of $\ln(I/I_0)$ vs. $\gamma^2\delta^2G^2[\Delta-(\delta/3)] \times 10^{10}$ ($\text{m}^{-2} \text{s}$) from PGSE NMR experiments (400 MHz, CD_2Cl_2 , 25 °C) for complex (\pm)-**4** (red), complex (\pm)-**1** (orange), complex (*R,R*)-**1** (yellow), complex (\pm)-**2** (green), proligand (\pm)- $\text{H}(\text{NNO}_{\text{SiPh}_3})$ (blue), proligand (\pm)- $\text{H}(\text{NNO}_{\text{Ad}})$ (purple) and internal standard tetrakis(trimethylsilyl)silane (TMSS) (black).

Procedure for calculating the diffusion coefficient and radii of a compound from PGSE NMR and X-ray data:

Equation 1 shows the relationship between the normalized intensity of the observed spin-echo signal (I/I_0) and the strength of the applied gradient (G) in a PGSE NMR experiment. The translational self-diffusion coefficient (D_t) of a species can therefore be calculated graphically from the slopes of the linear best-fit lines to the plots of $\ln(I/I_0)$ versus $\gamma^2\delta^2G^2[\Delta-(\delta/3)] \times 10^{10}$ ($\text{m}^{-2} \text{s}$) as γ , δ and Δ are all known constants.¹⁻³

$$(1) \quad I/I_0 = \exp[-D_t \gamma^2 \delta^2 G^2 [\Delta - (\delta/3)]]$$

where:

- I = intensity of the observed spin-echo
- I_0 = intensity of the observed spin-echo in the absence of a gradient
- γ = gyromagnetic ratio (for proton $2.675 \times 10^8 \text{ rad s}^{-1} \text{ T}^{-1}$)
- δ = length of the gradient pulse
- G = varied gradient strength
- Δ = delay between the midpoints of the gradients

In order to plot these graphs, the integration of a number of distinct and separate peaks in the ^1H NMR spectrum of the desired compound is first taken in the absence of a gradient (I_0) and then the integration is tracked as

a function of the gradient strength (I). The average I/I_0 values over this collection of peaks can be used to plot the graphs, as seen in Figure S10, for each compound. The average integration change for the internal standard (TMSS) can also be tracked as a function of the gradient strength, and the resulting D_t values from each experiment can be compared to the literature value ($13.8 \times 10^{-10} \text{ m}^2 \text{ s}^{-1}$) as a measure of the accuracy of the observed diffusion coefficients.³

The modified Stokes-Einstein equation (2) can be used to relate the D_t value of a compound to its hydrodynamic radius (r_H).³

$$(2) \quad D_t = \frac{k T}{c f \pi \eta r_H}$$

where: k = Boltzmann constant ($1.38 \times 10^{-23} \text{ m}^2 \text{ kg s}^{-1} \text{ K}^{-1}$)
 T = temperature (298.22 K)
 c = correction factor for compound size (depends on sample; TMSS, $c^{st} = 5.1$)
 f = correction factor for compound shape (depends on sample; TMSS, $f^{st} = 1$)
 π = the number pi (3.14159)
 η = fluid viscosity (for CH_2Cl_2 $\eta = 0.0004 \text{ kg s}^{-1} \text{ m}^{-1}$)

Equation (3) can be derived from this equation and used to relate the hydrodynamic radius of the sample multiplied by its size correction factor ($c^{sa} r_H^{sa}$) to the calculated diffusion coefficient of the sample (D_t^{sa}) and its shape correction factor (f^{sa}) and the diffusion coefficient, size and shape correction factors and hydrodynamic radius of the standard (TMSS), which are known from the literature.³ This procedure is used to eliminate the error associated with any experimental inconsistencies between different samples (such as concentration or temperature differences) as these would affect the internal standard in a similar manner (the concentration of the internal standard is kept constant between different experiments).

$$(3) \quad c^{sa} r_H^{sa} = \frac{D_t^{st} c^{st} f^{st} r_H^{st}}{D_t^{sa} f^{sa}}$$

The shape correction factor of the sample (f^{sa}), assuming a prolate ellipsoid shape for the molecule, can be calculated according to the literature based on the structural data from the x-ray crystal structure of the desired compound according to equation (4).³ The semi-major axis (a') is taken as half of the largest of the unit cell's measurements (a, b or c) and the semi-minor axis (b') is taken as the second largest unit cell measurement (a, b or c) divided by 2n (where n equals the number of molecules of interest occupying the unit cell).

$$(4) \quad f^{sa} = \frac{[1 - (b'/a')^2]^{1/2}}{(b'/a')^{2/3} \ln[(1 + [1 - (b'/a')^2]^{1/2}) / (b'/a')]}$$

Equation (5), reported by Chen and co-workers,⁴ can be used to plot a theoretical graph of $c r_H$ versus r_H using the radius of the particular solvent being used in the experiment (for CH_2Cl_2 $r_{\text{solv}} = 2.49 \text{ \AA}$). The equation of this graph is then used to calculate the r_H value of the sample, using the value of $c^{sa} r_H^{sa}$ calculated using the diffusion coefficient data.

$$(5) \quad c r_H = \frac{6 r_H}{1 + 0.695 (r_{\text{solv}}/r_H)^{2.234}}$$

The radius of a sample can also be calculated from the x-ray structural data assuming a spherical shape via equation (6). Note that for ease of calculation the volume occupied by any solvent molecules in the x-ray structures is not included in equation 6 but could be considered in order to give a more accurate volume for the molecule of interest ($V_{\text{molecule}} = [V - V_{\text{solvents}}]/n$).

$$(6) \quad r_{\text{x-ray}} = (3V/4\pi n)^{1/3} \quad \text{where: } \begin{array}{l} V = \text{volume of the unit cell} \\ n = \text{number of molecules in the unit cell} \end{array}$$

C. Characterization of compounds in the solid-state

Table S1. Crystallographic parameters of complexes **1**, **2**, **5** and **6**.

	(RR/SS)-1	(RR/SS)-2	(±)-5	(±)-6
empirical formula	C ₃₄ H ₃₉ Cl ₂ InN ₂ OSi	C ₂₄ H ₃₃ ClIn _{0.5} NO _{0.5}	C ₆₁ H ₉₇ Cl ₃ In ₂ N ₅ O ₃	C ₇₉ H ₁₀₃ Cl ₃ In ₂ N ₄ O ₃
Fw	705.48	426.86	1276.92	1486.63
T (K)	90	90	90	90
a (Å)	9.4897(10)	10.0632(12)	12.8751(10)	18.854(5)
b (Å)	12.2095(12)	14.7651(17)	15.9412(12)	11.886(4)
c (Å)	15.9328(16)	15.5923(19)	16.5097(12)	32.910(10)
α (deg)	105.831(2)	89.620(3)	64.991(2)	90
β (deg)	91.856(2)	73.121(3)	87.640(2)	100.603(7)
γ (deg)	111.387(2)	73.901(3)	87.658(2)	90
volume (Å ³)	1635.7(3)	2123.1(4)	3067.2(4)	7249(4)
Z	2	4	2	4
crystal system	triclinic	triclinic	triclinic	monoclinic
space group	P-1	P-1	P-1	P2 ₁ /n
d _{calc} (g/cm ³)	1.432	1.335	1.383	1.362
μ (MoKα) (cm ⁻¹)	9.52	7.19	9.29	7.97
2θ _{max} (deg)	60.16	61.324	60.52	61.192
absorption correction (T _{min} , T _{max})	0.8177, 0.8752	0.677, 0.806	0.7956, 0.8539	0.6469, 0.7461
total no. of reflections	108779	76944	173951	110250
no. of indep reflections (R _{int})	9600 (0.0378)	13104 (0.0662)	18161 (0.0559)	22143 (0.0708)
residuals (refined on F ² , all data): R ₁ ; wR ₂	0.0292, 0.0572	0.0381, 0.0505	0.0417, 0.0766	0.0554, 0.0750
GOF	1.066	0.926	1.021	1.026
no. observations [I > 2s(I)]	9600	13104	18161	22143
residuals (refined on F ²): R ₁ ^a ; wR ₂ ^b	0.0228, 0.0537	0.0282, 0.0486	0.0294, 0.0719	0.0353, 0.0679

^a R₁ = Σ ||F_o - |F_c|| / Σ |F_o|; ^b wR₂ = [Σ(w(F_o² - F_c²)²)/Σw(F_o²)²]^{1/2}

D. Kinetic studies of the polymerization of lactide by catalysts 4-6

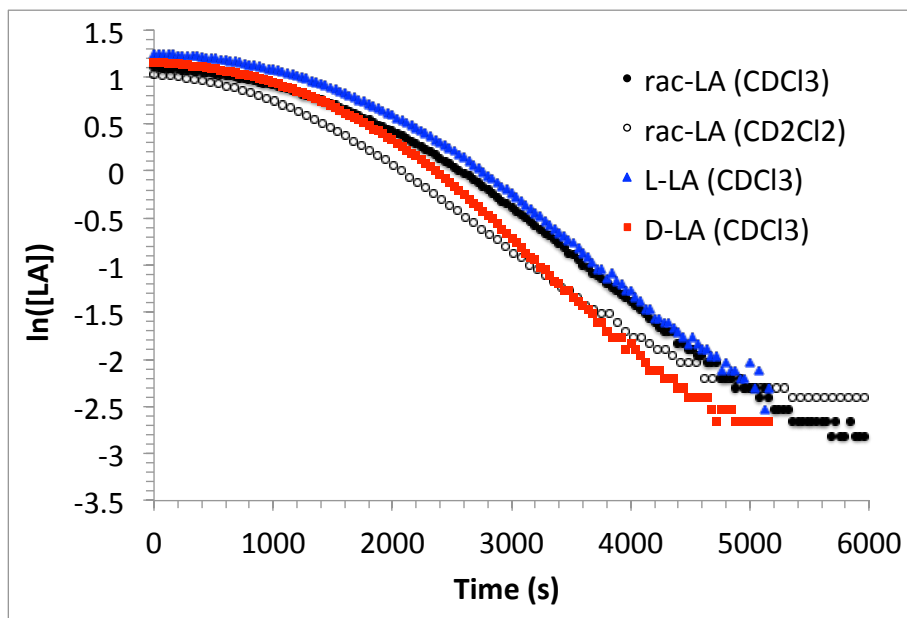


Figure S11. Plots of the $\ln([LA])$ vs. time for the polymerization of *rac*-, L- and D-LA (0.5 M) by complex (\pm)-4 (2.4 mM) monitored to >97% conversion by 1H NMR spectroscopy in $CDCl_3$ and CD_2Cl_2 with 1,3,5-trimethoxybenzene used as an internal standard (0.03 M).

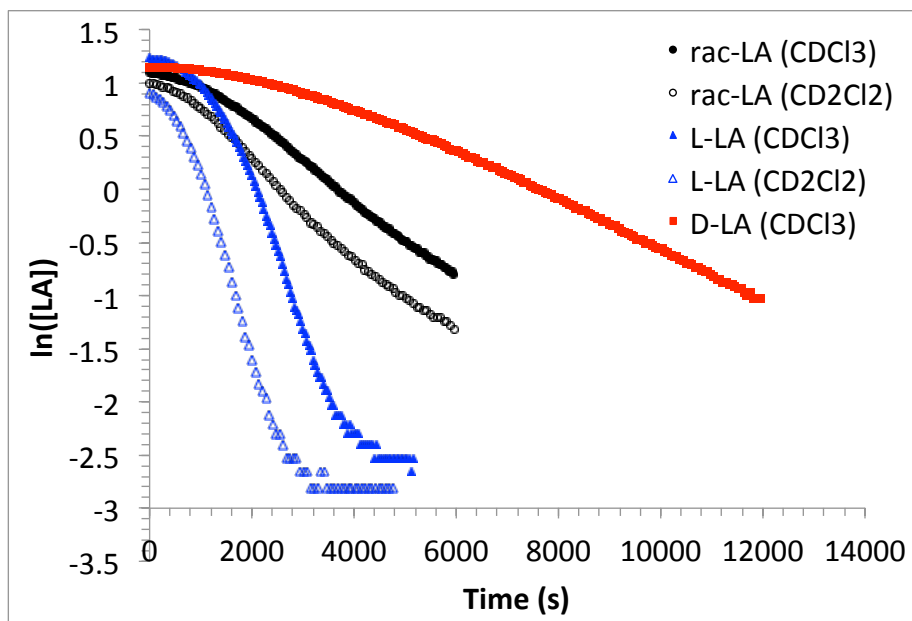


Figure S12. Plots of the $\ln([LA])$ vs. time for the polymerization of *rac*-, L- and D-LA (0.5 M) by complex (*R,R*)-4 (2.4 mM) monitored to >86% conversion by 1H NMR spectroscopy in $CDCl_3$ and CD_2Cl_2 with 1,3,5-trimethoxybenzene used as an internal standard (0.03 M).

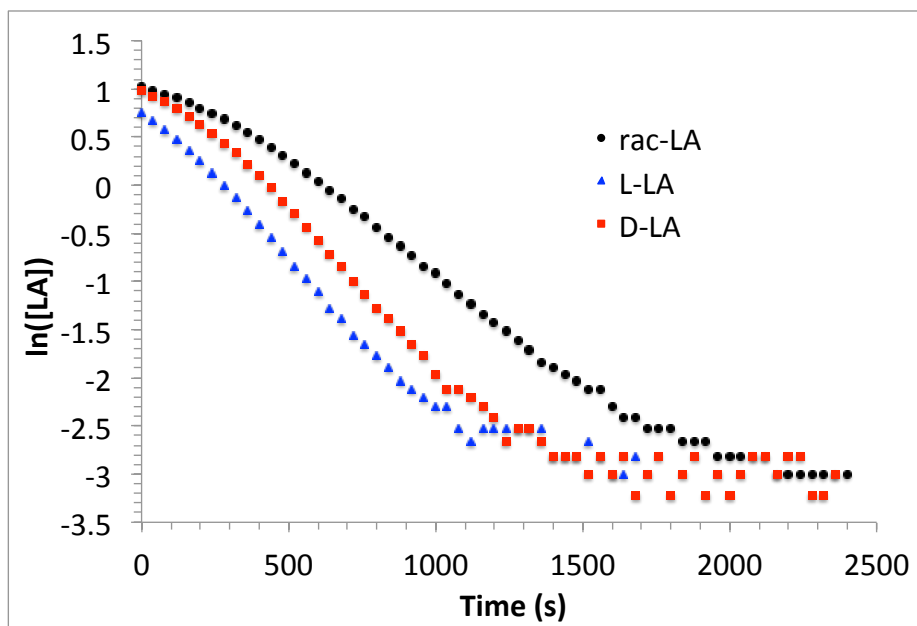


Figure S13. Plots of the $\ln([LA])$ vs. time for the polymerization of *rac*-, L- and D-LA (0.5 M) by complex (\pm)-**5** (2.4 mM) monitored to >98% conversion by ^1H NMR spectroscopy in CDCl_3 with 1,3,5-trimethoxybenzene used as an internal standard (0.03 M).

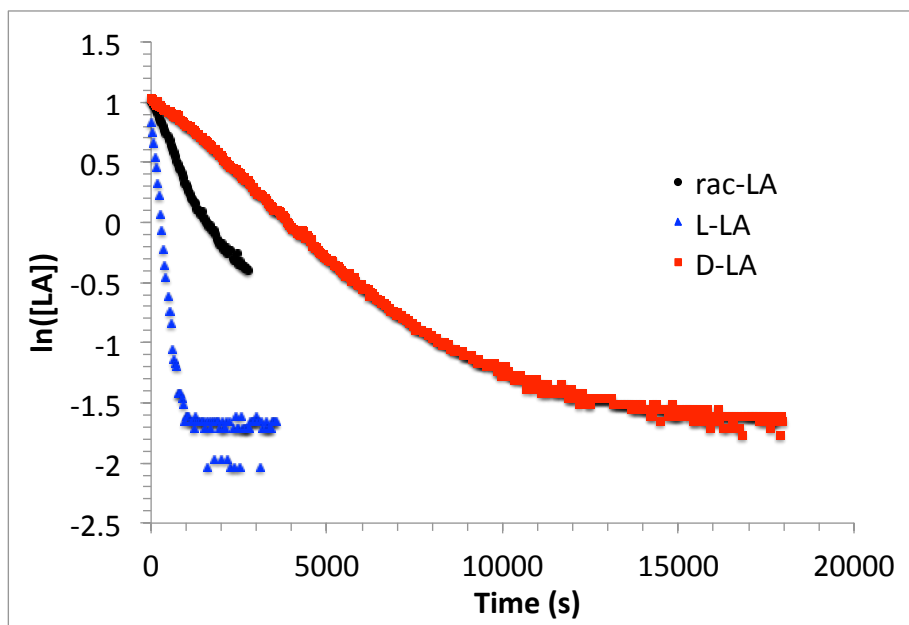


Figure S14. Plots of the $\ln([LA])$ vs. time for the polymerization of *rac*-, L- and D-LA (0.5 M) by complex (*R,R*)-**5** (2.4 mM) monitored to >80% conversion by ^1H NMR spectroscopy in CDCl_3 with 1,3,5-trimethoxybenzene used as an internal standard (0.03 M).

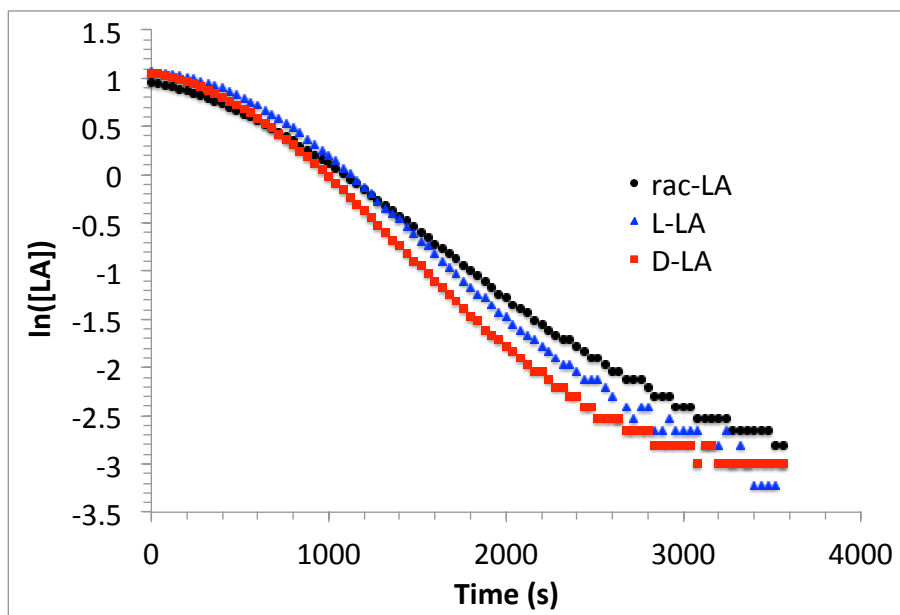


Figure S15. Plots of the $\ln([LA])$ vs. time for the polymerization of *rac*-, L- and D-LA (0.5 M) by complex (\pm)-**6** (2.4 mM) monitored to >98% conversion by ^1H NMR spectroscopy in CDCl_3 with 1,3,5-trimethoxybenzene used as an internal standard (0.03 M).

E. *In situ* ^1H NMR spectroscopy of the polymerization of lactide by catalysts 4-6

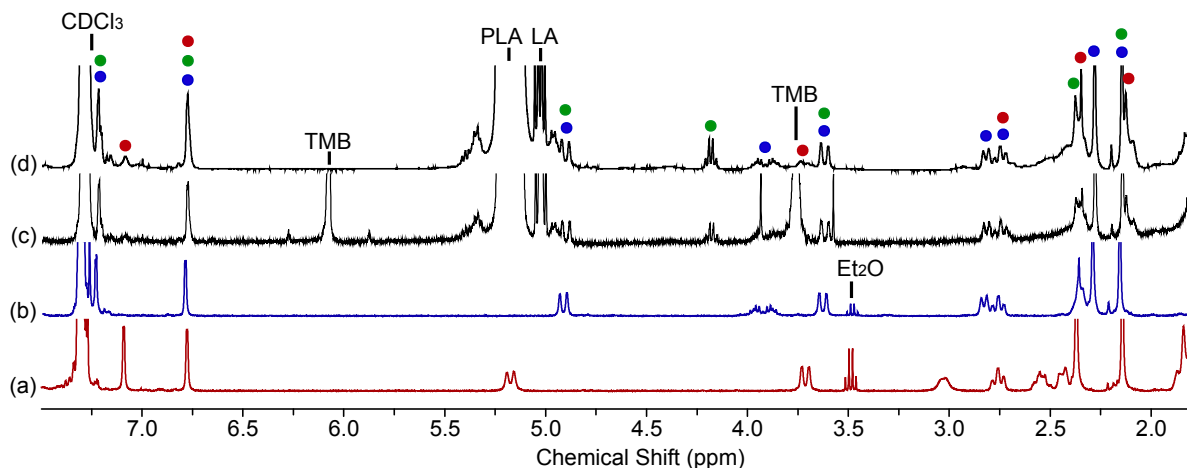


Figure S16. ^1H NMR spectra (400 MHz, CDCl_3 , 25 °C) of (a) complex (±)-1, (b) complex (±)-4, (c) the polymerization of *rac*-LA (0.48 M) by complex (±)-4 (2.4 mM) in CDCl_3 monitored *in situ* in an NMR tube to 97% conversion with 1,3,5-trimethoxybenzene (TMB) used as an internal standard and (d) the polymerization of *rac*-LA (~0.5 M) by complex (±)-4 (~2 mM) which was stirred at room temperature in CDCl_3 for 2 hours before being analyzed by NMR spectroscopy (98% conversion). The blue dots denote peaks coincident with (±)-4, the red dots denote peaks coincident with (±)-1 and the green dots denote the indium polymeryl species.

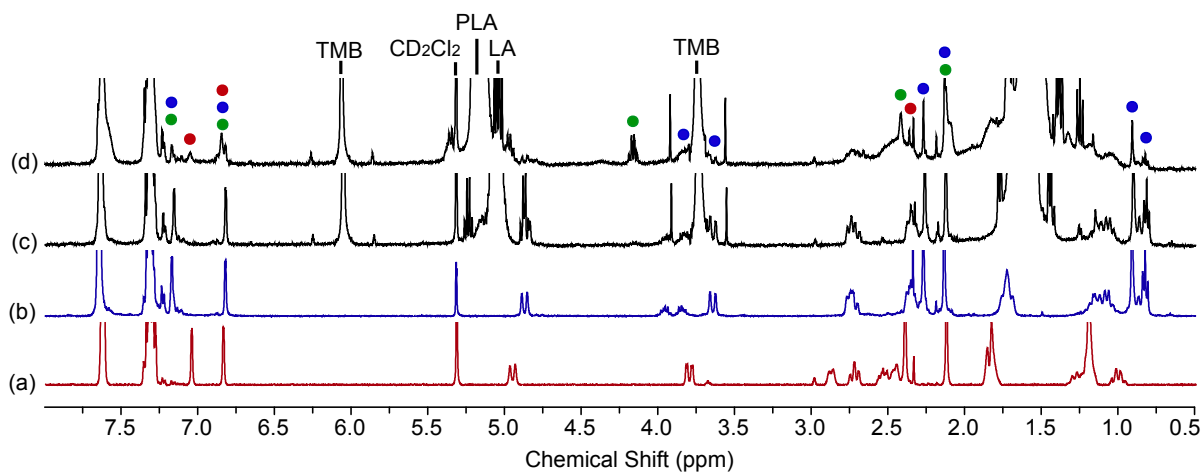


Figure S17. ^1H NMR spectra (400 MHz, CD_2Cl_2 , 25 °C) of (a) complex (±)-1, (b) complex (±)-4 and the polymerization of *rac*-LA (0.48 M) by complex (±)-4 (2.4 mM) in CD_2Cl_2 monitored *in situ* in an NMR tube with 1,3,5-trimethoxybenzene (TMB) used as an internal standard at 1% (c) and 97% (d) conversion. The blue dots denote peaks coincident with (±)-4, the red dots denote peaks coincident with (±)-1 and the green dots denote the indium polymeryl species.

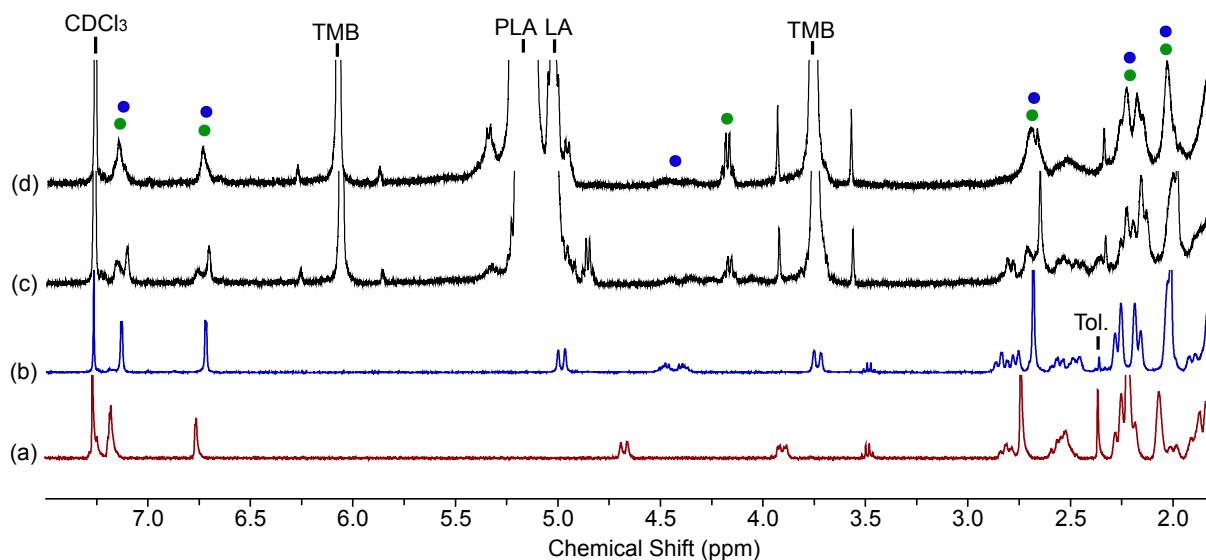


Figure S18. ^1H NMR spectra (400 MHz, CDCl_3 , 25 $^\circ\text{C}$) of (a) complex (\pm)-2, (b) complex (\pm)-5 and the polymerization of *rac*-LA (0.48 M) by complex (\pm)-5 (2.4 mM) in CDCl_3 monitored *in situ* in an NMR tube with 1,3,5-trimethoxybenzene (TMB) used as an internal standard at 29% (c) and 97% (d) conversion. The blue dots denote peaks coincident with (\pm)-5 and the green dots denote the indium polymeryl species.

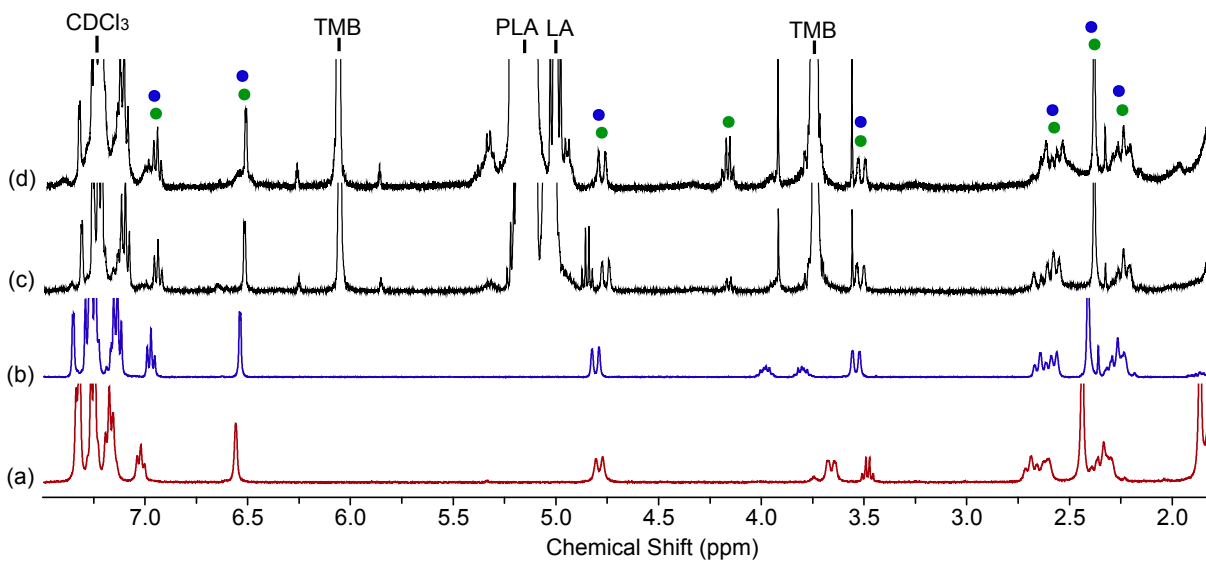


Figure S19. ^1H NMR spectra (400 MHz, CDCl_3 , 25 $^\circ\text{C}$) of (a) complex (\pm)-3, (b) complex (\pm)-6 and the polymerization of *rac*-LA (0.48 M) by complex (\pm)-6 (2.4 mM) in CDCl_3 monitored *in situ* in an NMR tube with 1,3,5-trimethoxybenzene (TMB) used as an internal standard at 29% (c) and 97% (d) conversion. The blue dots denote peaks coincident with (\pm)-6 and the green dots denote the indium polymeryl species.

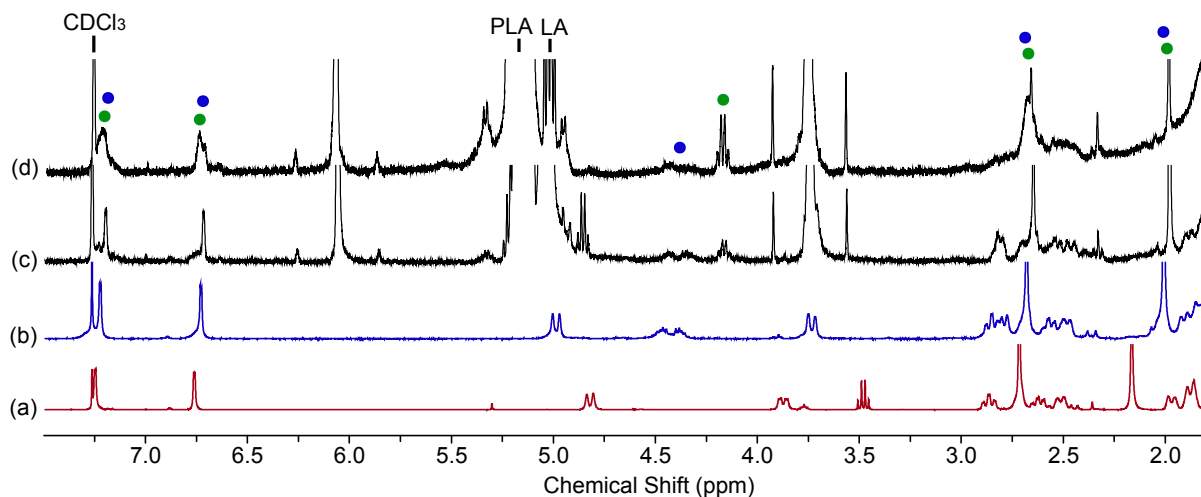
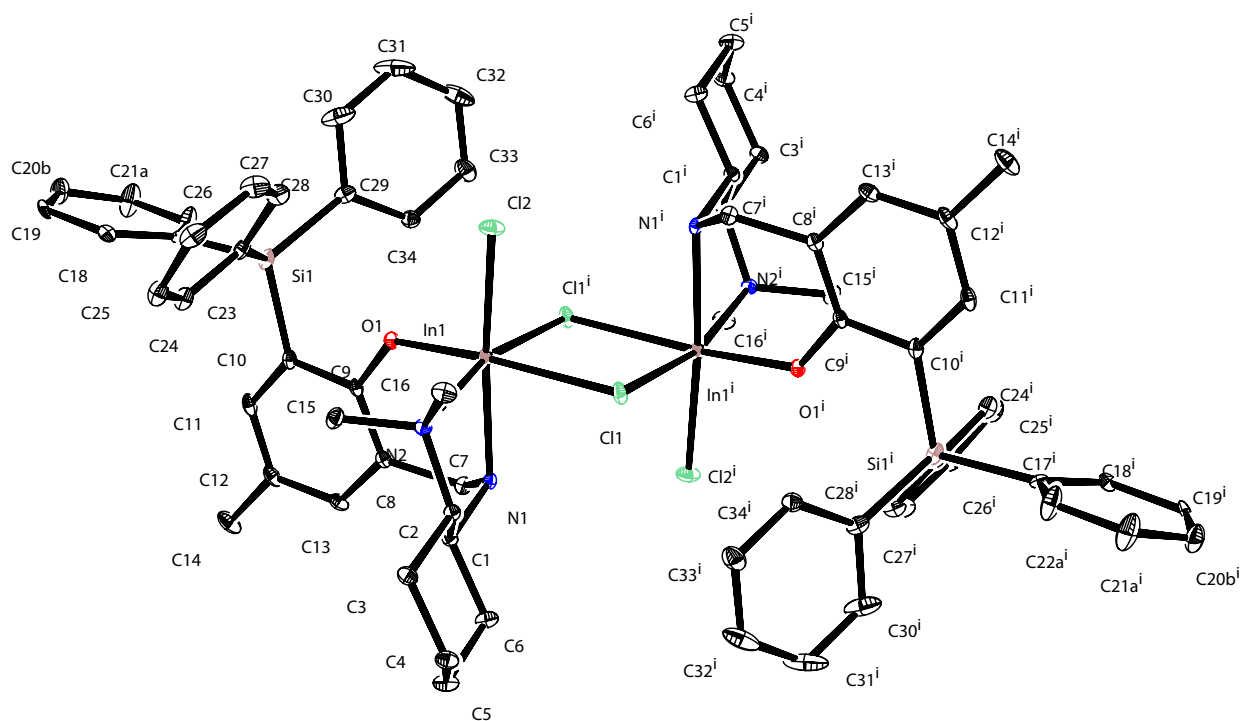
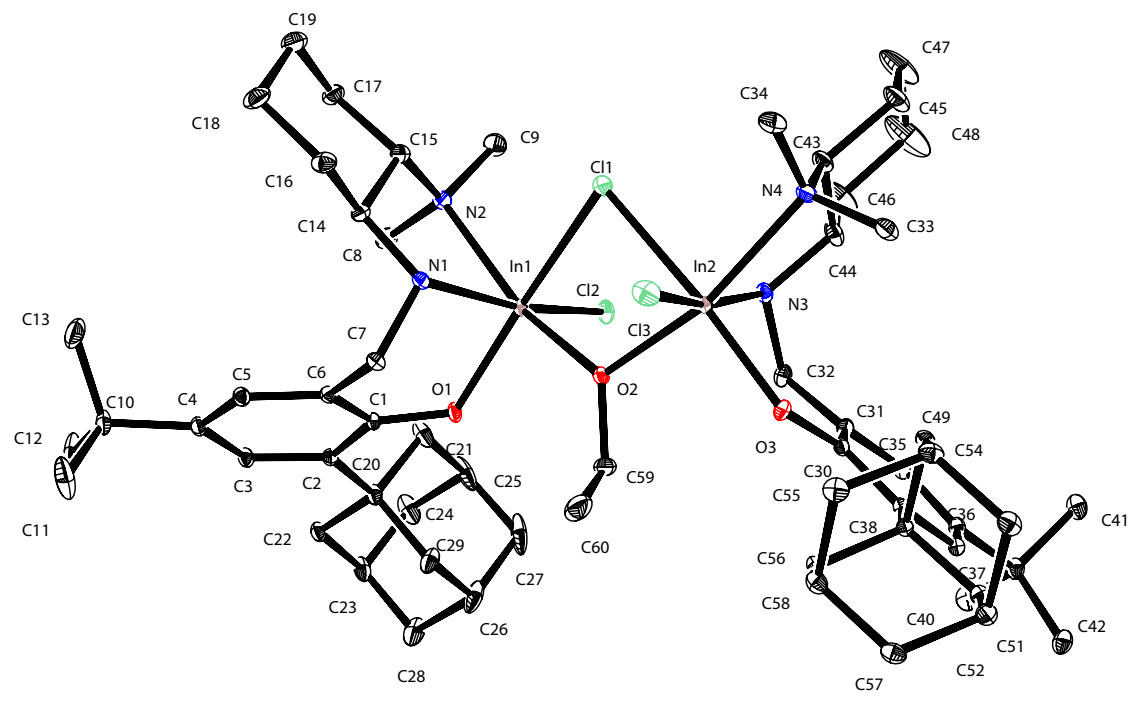
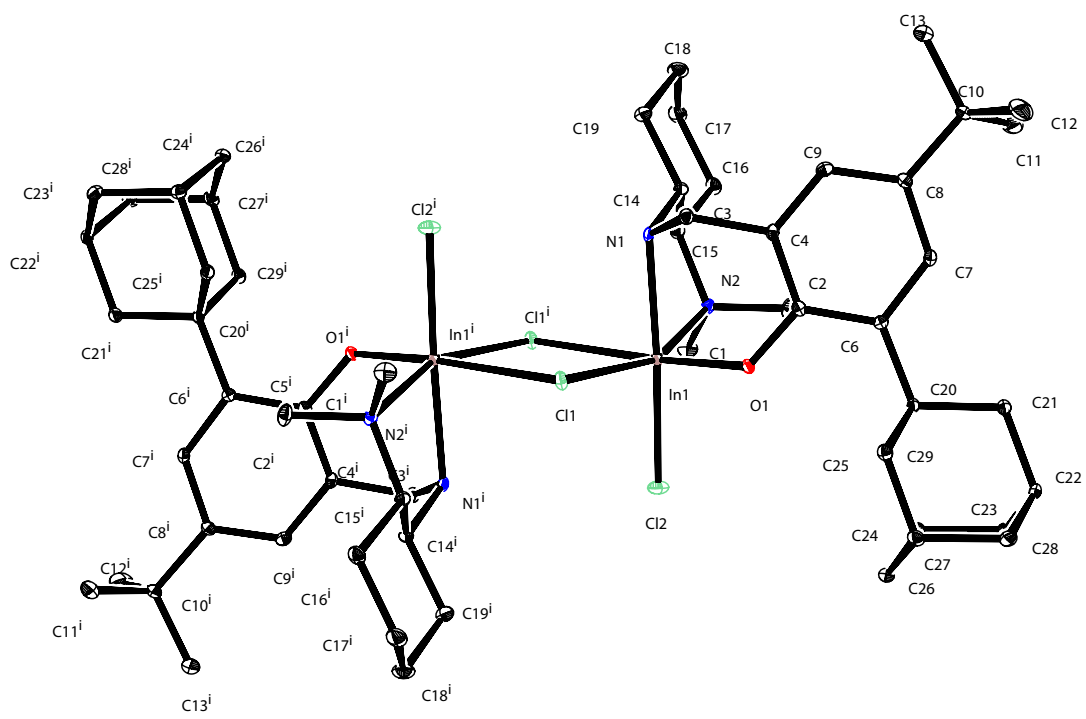
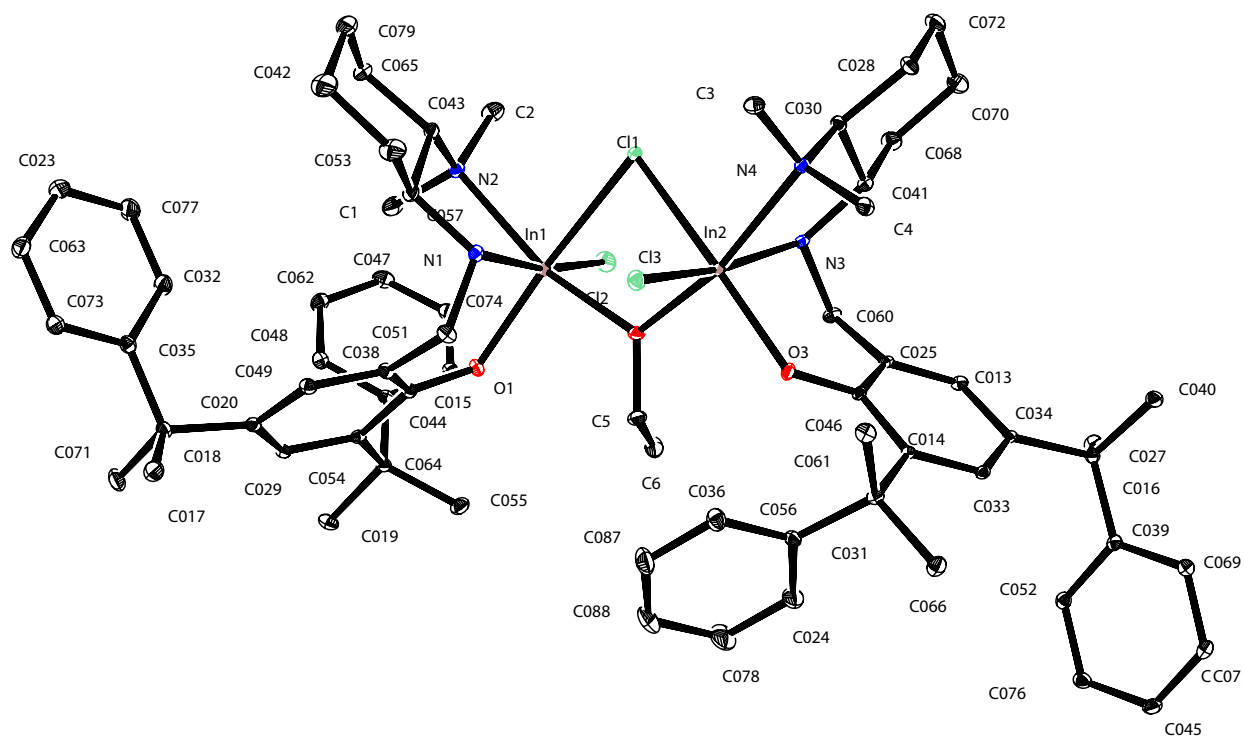


Figure S20. ^1H NMR spectra (400 MHz, CDCl_3 , 25 $^\circ\text{C}$) of (a) complex $(\pm)\text{-(NNO}_{t\text{Bu}})\text{InCl}_2$, (b) complex $(\pm)\text{-}[(\text{NNO}_{t\text{Bu}})\text{InCl}]_2(\mu\text{-Cl})(\mu\text{-OEt})$ and the polymerization of *rac*-LA (0.48 M) by complex $(\pm)\text{-}[(\text{NNO}_{t\text{Bu}})\text{InCl}]_2(\mu\text{-Cl})(\mu\text{-OEt})$ (2.4 mM) in CDCl_3 monitored *in situ* in an NMR tube with 1,3,5-trimethoxybenzene (TMB) used as an internal standard at 29% (c) and 97% (d) conversion. The blue dots denote peaks coincident with $(\pm)\text{-}[(\text{NNO}_{t\text{Bu}})\text{InCl}]_2(\mu\text{-Cl})(\mu\text{-OEt})$ and the green dots denote the indium polymeryl species.

F. Fully-labelled ORTEP diagrams of solid state structures of complexes 1, 2, 5, and 6







G. References

1. M. Valentini, H. Ruegger and P. S. Pregosin, *Helv. Chim. Acta*, 2001, **84**, 2833-2853.
2. C. M. Silvernail, L. J. Yao, L. M. R. Hill, M. A. Hillmyer and W. B. Tolman, *Inorg. Chem.*, 2007, **46**, 6565-6574.
3. A. Macchioni, G. Ciancaleoni, C. Zuccaccia and D. Zuccaccia, *Chem. Soc. Rev.*, 2008, **37**, 479-489.
4. H. C. Chen and S. H. Chen, *J. Phys. Chem.*, 1984, **88**, 5118-5121.